MACROSCALE THALAMIC FUNCTIONAL ORGANIZATION DISTURBANCES AND UNDERLYING CORE CYTOARCHITECTURE IN EARLY-ONSET SCHIZOPHRENIA

Running title: Expansion of thalamic functional hierarchies in schizophrenia

Yun-Shuang Fan [1,2], Yong Xu [3], Şeyma Bayrak [2], James M. Shine [6], Haoru Li [1], Liang Li [1,7], Siqi Yang [1], Yao Meng [1], Sofie Louise Valk [2,5*#], Huafu Chen [1,4*#]

1. The Clinical Hospital of Chengdu Brain Science Institute, School of Life Science and Technology, University of Electronic Science and Technology of China, Chengdu, China; 2. Otto Hahn Group Cognitive Neurogenetics, Max Planck Institute for Human Cognitive and Brain Sciences, Leipzig, Germany; 3. Department of Psychiatry, First Hospital/First Clinical Medical College of Shanxi Medical University, Taiyuan, China; 4. MOE Key Lab for Neuroinformation, High-Field Magnetic Resonance Brain Imaging Key Laboratory of Sichuan Province, University of Electronic Science and Technology of China, Chengdu, China; 5. Institute of Neuroscience and Medicine (INM-7: Brain and Behavior), Research Centre Jülich, Jülich, Germany; 6. Brain and Mind Center, The University of Sydney, Sydney, Australia; 7. Academy for Advanced Interdisciplinary Studies, Peking University.

* Both last co-authors contributed equally.

Corresponding authors:
Huafu Chen, E-mail: chenhf@uestc.edu.cn & Sofie Louise Valk, E-mail: valk@cbs.mpg.de.

Title character count: 111
Running title character count: 55
Word count of abstract: 181
Word count of text body: 4838
Number of references: 57
Number of tables: 0
Number of figures: 4 (All colored)
Supplement material: 1

Abstract

Schizophrenia is a polygenetic mental disorder with a heterogeneous clinical presentation, and is associated with an abnormal connectivity profile in the cortex. The thalamus acts as an integrated hub in cortical function and plays a central role in the development of the cerebral cortex. Thus, altered functional organization of the thalamus might account for overarching cortical disruptions in schizophrenia. Here, we contrasted resting-state fMRI in 99 antipsychotic-naive first-episode early-onset schizophrenia (EOS) patients and 100 typically developing controls to study whether macroscale thalamic organization is altered in EOS. Employing manifold learning techniques on thalamocortical functional connectome, we derived both lateral-medial and anterior-posterior gradient axes of the thalamus. We observed increased dispersion of macroscale thalamic functional organization in EOS patients, which was related to altered thalamocortical interactions both in unimodal and transmodal networks. Moreover, using an *ex vivo* approximation of core-matrix cell distribution, we found that core cells particularly underlie the macroscale abnormalities in EOS patients. Last, functional decoding indicated that schizophrenia-related abnormalities in connectome-gene couplings were associated with both perceptual and abstract cognitive functions, suggesting a unitary pathophysiology of diverse symptoms in schizophrenia.

Keywords: *connectome; cytoarchitectural; early-onset schizophrenia; functional hierarchy; thalamus.*

Introduction

Schizophrenia is a polygenetic psychiatric illness characterized by anomalies in thoughts, perceptions, and behaviors, which usually emerge during early adulthood (Kinney & Matthysse, 1978). Over the past two decades, a wealth of neuroimaging studies has indicated that schizophrenia can be associated with pathological interactions across widely distributed brain regions, instead of focal brain damages. Accordingly, the overarching dysconnection hypothesis posits that schizophrenia results from brain structural and functional connectivity abnormalities (Stephan, Friston, & Frith, 2009). The thalamus, which is well-placed to arbitrate the interactions between distributed brain organization (Shine, 2021), might play a pivotal role in the pathophysiological process of schizophrenia (Jones, 1997; Pergola, Selvaggi, Trizio, Bertolino, & Blasi, 2015).

The thalamus is a cytoarchitecturally heterogeneous diencephalic structure that contains an admixture of Parvalbumin (PVALB)-rich ‘Core’ cells and Calbindin (CALB1)-rich ‘Matrix’ cells (Jones, 2009). Whereas core cells send targeted projections to granular layers (Layers III and IV) of unimodal primary regions, such as primary visual, auditory and somatosensory cortices, matrix cells preferentially target supragranular layers (Layers I-III) over wide areas in a diffuse pattern (Jones, 2001). This means that distinct thalamic cells may interact with cortical areas organized into different topological zones (Muller et al., 2020). Cellular-scale information of the thalamus may be a critical factor to understand the thalamocortical interactions that supports cognition and behavior. Indeed, the thalamocortical system has been suggested to form the basis for binding multiple sensory

experiences into a single framework of consciousness (Jones, 1998). By coordinating the modular architecture of cortical networks, the thalamus has been reported to be engaged in integrating information processing within the whole cerebral cortex (Hwang, Bertolero, Liu, & D'Esposito, 2017).

In accordance with its function coordinating cortical network organization, the thalamus plays the central role in the development of the cerebral cortex (Lopez-Bendito & Molnar, 2003). During childhood and adolescence, the thalamus develops in concordance with the cerebral cortex and disturbances of this coordinated development relate to psychotic symptomatology, such as cognitive dysfunctions (Nakagawa, 2019), serving as a precursor of schizophrenia. Indeed, thalamocortical dysconnectivity patterns, characterized by hypoconnectivity with prefrontal regions and hyperconnectivity with sensorimotor areas, have been reported in both pediatric (M. Zhang et al., 2021) and early-stage (Woodward & Heckers, 2016) patients with schizophrenia. The dysconnectivity pattern has been hypothesized to arise from disturbed brain maturation, particularly during the transition from youth to adulthood (Woodward, Karbasforoushan, & Heckers, 2012). Intriguingly, thalamo-prefrontal hypoconnectivity and thalamo-sensorimotor hyperconnectivity is correlated in patients, potentially implying a shared pathophysiological mechanism (Woodward & Heckers, 2016). However, few studies have investigated thalamocortical connectome in the still developing brain of schizophrenia from a comprehensive perspective.

Recently, the application of manifold learning techniques has emerged as a promising strategy for holistic representations of brain connectivity. These novel data-driven connectome-wide methods decompose high dimensional connectomes into a series of low dimensional axes recapitulating spatial gradients of connectivity variations (Margulies et al., 2016; Paquola et al., 2019). The gradient framework describes a continuous coordinate system, which are in contrast to previous clustering-based methods resulting in discrete communities (Hong et al., 2019). Using these methods in the context of cortex-wide functional connectomes, previous studies observed a cortical hierarchy that spans from unimodal primary regions to transmodal regions (Vazquez-Rodriguez et al., 2019), which has a close link with cortical microstructure like cytoarchitecture or myeloarchitecture (Huntenburg, Bazin, & Margulies, 2018). Their coupling along the unimodal-transmodal axis has been reported to be genetically- and phylogenetically-controlled, supporting flexible cognitive functions in primates (Valk et al., 2021). Perturbed macroscale cortical functional hierarchies have been reported in various neurological (Bayrak et al., 2019; Meng et al., 2021) and psychiatric disorders (Hong et al., 2019) including schizophrenia (D. Dong et al., 2020). Also, thalamic hierarchies have been previously derived from thalamocortical connectome, identifying a lateral-medial (L-M) principal gradient and an anterior-posterior (A-P) secondary gradient (Yang et al., 2020). The L-M axis captures thalamic anatomical nuclei differentiation, while the A-P axis characterizes unimodal-transmodal functional communities and cognitive ontologies. Also the functional connectivity projection of core and matrix cells to the cortex has been shown to recapitulate the unimodal-transmodal cortical gradients, and argued to play a major role in shaping functional dynamics within the

cerebral cortex (Muller et al., 2020). Given the possible implication of the thalamus in schizophrenia, thalamic hierarchies may be altered and could provide new insights into the disruptions in the thalamocortical system in schizophrenia.

Here, we leveraged a cohort of individuals with early-onset schizophrenia (EOS), a disorder that is neurobiologically continuous with its adult counterpart (Jacobsen & Rapoport, 1998), to examine whether macroscale thalamic functional organization shows disturbances in the still developing brain of schizophrenia, mirroring neocortical reports. To this end, we first evaluated functional hierarchies of the thalamus by employing manifold learning techniques on thalamocortical functional connectivity (Coifman & Lafon, 2006). We then embedded thalamic functional hierarchies in a neurobiological context by spatially correlating the macroscale patterns with gene expression maps of PVALB and CALB1 from the Allen Human Brain Atlas (AHBA) (Hawrylycz et al., 2012).

Results

Thalamic connectome manifolds in TD and EOS

The principal gradient (G1) of the thalamus revealed a L-M axis, and the second gradient (G2) described an A-P axis, in line with previous work (Yang et al., 2020). In EOS patients, we observed expansions at both anchors of the G1; the lateral portions including the ventral lateral and ventral posterior thalamic nuclei, the medial dorsal areas compared to TD controls (**Figure 1A**, TFCE, $p < 0.005/2$). We also observed expansions along the G2 axis including the pulvinar and anterior nuclear groups (**Figure 1B**, TFCE, $p < 0.005/2$). Combing G1 and G2 axes, we computed an eccentricity score using the square root of the Euclidian distance from each thalamic voxel to the center of mass in the two-dimensional gradient space (Park et al., 2021). Global eccentricity was assessed for each participant by averaging eccentricity values across all thalamic voxels. We found significantly increased global eccentricity for thalamic voxels in EOS compared to TD ($t = 2.34$, $p = 0.02$), indicating an expansion of macroscale thalamic functional organization in patients (**Figure 1C**).

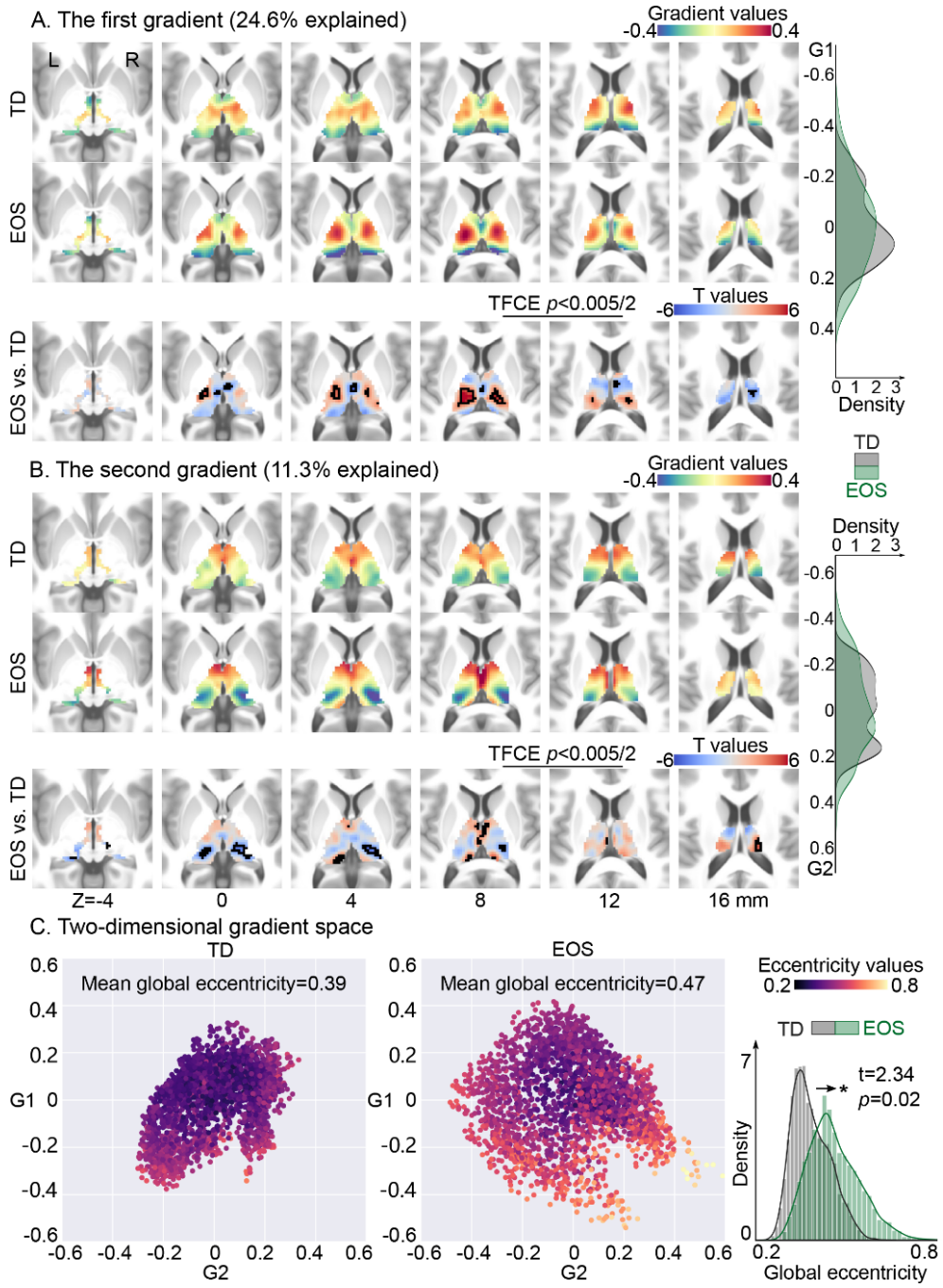

Figure 1. Thalamic connectome manifolds in typically developing (TD) controls and early-onset schizophrenia (EOS) patients. **(A)** The group-level primary gradients (G1) for TD and EOS, and their between-group differences. The G1 depicts a transition from lateral to medial portions of the thalamus. Thalamic voxels showing significant G1 score differences were surrounded by black contours [t-test, EOS vs. TD; threshold-free cluster enhancement (TFCE), $p < 0.005$]. The density map represents the distribution of G1 loading for EOS (green) or TD (gray). **(B)** The group-level secondary gradients (G2) for TD and EOS, and their differences. G2 separates the anterior thalamic portions from the posterior

portions. Thalamic voxels with significant G2 differences were surrounded by black contours. The density map represents the G2 loading for EOS (green) or TD (gray). (**C)** Gradient spaces built on the group-level G1 and G2, separately for TD and EOS. Each point represents a thalamic voxel embedded in the gradient space. Voxels are color coded based on their mean eccentricity scores across subjects. Higher eccentricity indicates higher dispersion in the gradient space. The density plot depicts the distribution of eccentricity scores in EOS and TD

Functional community relevance of thalamic gradients

Utilizing a whole-brain canonical network parcellation (Yeo et al., 2011), thalamocortical functional connectome was distributed into six functional communities (**Figure 2A**). To study the network-level relevance of connectome gradients, we averaged gradient loadings within each network for each subject. Gradient scores within each network were then compared between the EOS and TD groups (**Figure 2B**, Bonferroni correction, $p < 0.05/6$). EOS Patients had significantly higher mean G1 scores in the SMN ($t = 5.37$, $p < 0.0001$) and DAN ($t = 2.94$, $p = 0.004$), and lower G1 scores in the VAN ($t = -2.85$, $p = 0.005$), FPN ($t = -3.69$, $p = 0.0003$), and DMN ($t = -3.03$, $p = 0.003$) relative to TD controls. For the G2 axis, patients showed decreased gradient scores in the VIS ($t = -4.08$, $p < 0.0001$), and increased in the DMN ($t = 5.45$, $p < 0.0001$). Network level gradient score differences were then projected onto the two-dimensional gradient space for TD and EOS (**Figure 2C**). These projections revealed that EOS patients had apparent dissociation of SMN-related thalamic voxels along the G1 axis, and a larger dissociation of VIS- and DMN-related regions along the G2 axis.

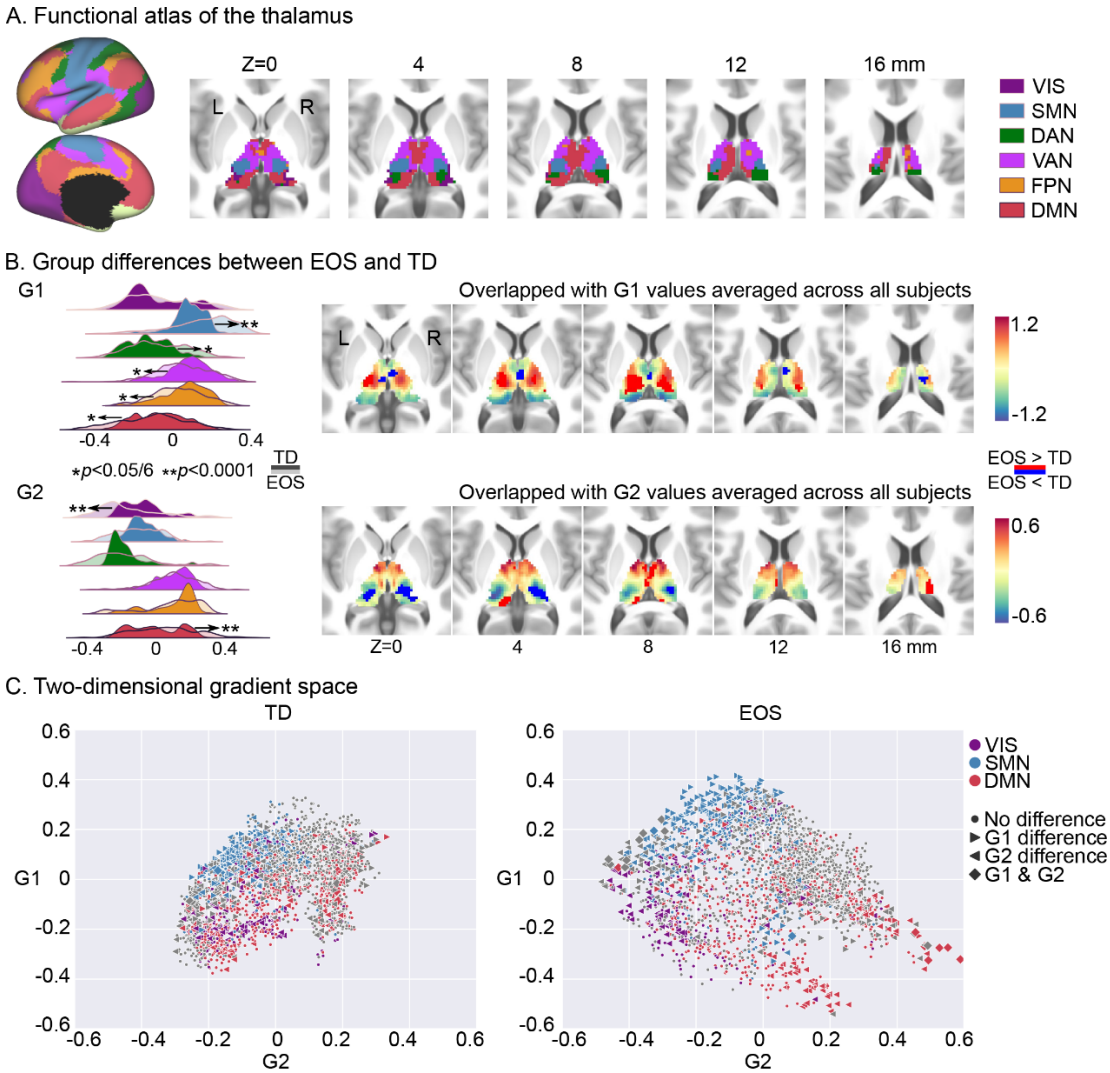

Figure 2. Thalamocortical connectome manifolds distributed into functional communities. (A) Network-level representations of the thalamocortical connectome. (**B)** G1 and G2 scores depicted within functional communities. Density maps indicate mean gradient scores (top left: G1, bottom left: G2) within six networks for EOS and TD. Network level differences between EOS and TD were accessed by t-tests, and significant differences depicted by * (Bonferroni correction, $p < 0.05$) and ** ($p < 0.0001$). Thalamic G1 (top right) and G2 (bottom right) representations across all participants. Voxels showing higher gradient values in EOS are colored red, whereas voxels with lower gradient values are colored blue. (**C)** Gradient space representation of the thalamus together with functional communities for TD (left) and EOS (right). Thalamic voxels are situated based on their G1 (x-axis) and G2 (y-axis) scores are colored according to their network assignment (purple-VIS; blue-SMN; red-DMN; grey-all other networks). ► stands for the G1 score differences between EOS and TD; ◄ for the G2 score differences; ♦ for both G1 and G2 score differences; ● for no difference. VIS, the visual network; SMN, the sensorimotor network; DAN, the dorsal attention network; VAN, the ventral attention network; FPN, the frontoparietal network; DMN, the default mode network.

The core-matrix cytoarchitecture in the thalamus

Having established macroscale thalamic connectome manifolds, we further investigated whether connectome differences between patients and controls were specific to thalamic cytoarchitectural features, namely core vs. matrix cells. Thus, mRNA expression levels for CALB1 (core type cells) and PVALB (matrix type cells) were separately assessed at the thalamic voxel level (**Figure 3A**). The differential expression level between CALB1 and PVALB, i.e., CPt scores, was used to delineate thalamic core/matrix type cell distribution, where positive/negative CPt value indicated with matrix/core cell type, respectively. Manifold eccentricity was used to evaluate the gradient space-embedded position of each thalamic voxel. EOS patients showed increased eccentricity in medial dorsal, ventral lateral, and ventral anterior nucleus compare to TD controls, indicating their increased dispersion from the center of the manifold (TFCE, $p < 0.005$). We then mapped the core-matrix cytoarchitectural features onto the two-dimensional gradient space (**Figure 3B**). Patients' core cells showed mildly increased global eccentricity compared with core cells of TD ($t = 2.38$, $p = 0.02$), but matrix cells did not ($t = 1.62$, $p = 0.11$). No significant difference was found between global eccentricity of core and matrix populations within EOS ($t = 1.07$, $p = 0.29$) or TD ($t = 0.36$, $p = 0.72$). Next, Pearson's correlations were used to quantified group-level associations between the cytoarchitecture and the connectome manifold disturbances, and the variogram methods that controls for the spatial autocorrelations were used to determined statistical significance levels (**Figure 3C**). A negative correlation was found between CPt values and t values of eccentricity ($r = -0.29$, $p_{vario} = 0.002$). In detail, increased dispersion of macroscale connectome gradient space in patients was particularly

related to core cells (r = 0.31, $p_{vario} < 0.0001$), rather than matrix cells (r = 0.02, $p_{vario} = 0.84$).

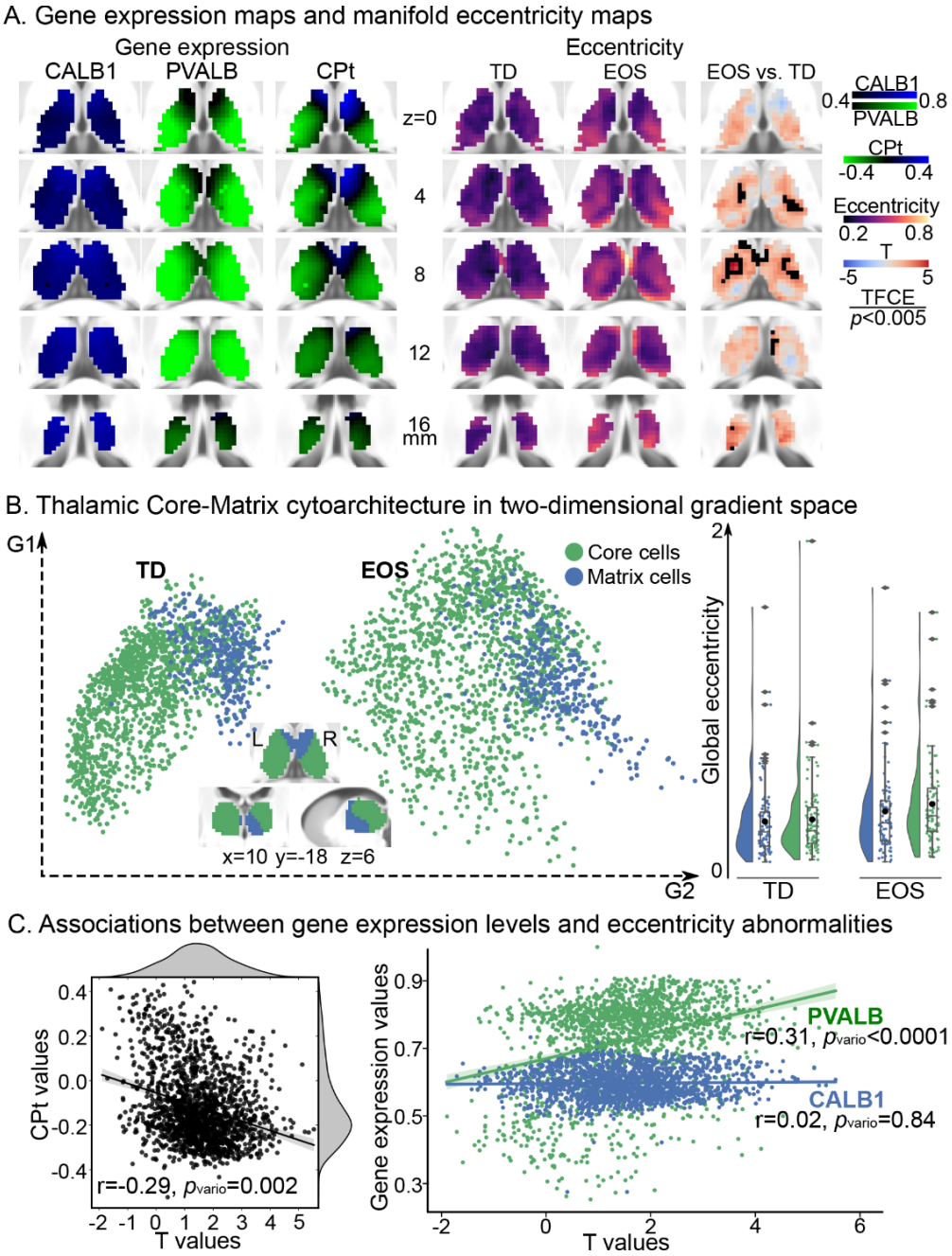

Figure 3. The core-matrix cytoarchitecture of the thalamus. (A) mRNA expression levels for Calbindin (CALB1) and Parvalbumin (PVALB) proteins, and eccentricity scores for thalamic voxels. CPt denotes the differential gene expression level for CALB1 and PVALB. Thalamic voxels with positive CPt values (blue) indicate matrix projection cells, and negative CPt values (green) related to core populations. Eccentricity scores of thalamic voxels are depicted for TD and EOS, and their differences are assessed by t-tests (EOS vs.

TD). Voxels with significant eccentricity differences are surrounded by black contours (TFCE, $p < 0.005$). **(B)** Core-matrix cytoarchitectural features of thalamic voxels projected onto the two-dimensional gradient space for TD and EOS. Rainclouds present group comparisons of global eccentricity in four fashions: global eccentricity values across core cells in EOS vs. global eccentricity values across matrix cells in EOS; core cells in TD vs. matrix cells in TD; core cells in EOS vs. core cells in TD; matrix cells in EOS vs. matrix cells in TD. (C) Associations between eccentricity differences (t values; EOS vs. TD) and differential gene expression levels (CPt, left) as well as single gene expression levels (CALB1 and PVALB, right). Correlations were obtained across thalamic voxels (Pearson r values) and their significances were tested using variogram approach (p_{vario} values).

Cognitive implications of gene-connectome couplings

Given the association between CPt map and thalamocortical connectome, we further assessed whether gene-connectome coupling contributes to cognitive processing. Thus, we projected the core-matrix cytoarchitecture to the cerebral cortex and then conducted a meta-analysis using the NeuroSynth database (Yarkoni, Poldrack, Nichols, Van Essen, & Wager, 2011). Couplings between functional connectome and gene expression (i.e., CPc maps) were computed and further down sampled into 400 cortical parcels. Core cell populations were mainly associated with unimodal regions that subserve primary sensory and multisensory functions. Matrix cell populations were associated with transmodal cortices characterized by more abstract cognition (See **Figure S1** for detailed meta-analysis results). Compared with TD controls, EOS patients showed CPc increases in the DMN including the inferior parietal lobule, posterior cingulate cortex, inferior prefrontal cortex, temporal areas, and the FPN including the precuneus and inferior parietal sulcus, and temporoparietal junction network (**Figure 4A,** FDR, $p < 0.005$). Abnormal CPc increases were associated with seven cognitive topics including declarative memory, autobiographical memory, working memory, verbal semantics, social cognition, language, and visuospatial (z−statistic > 3.1), indicating its implications in higher-level cognitive processes. Additionally, CPc reductions were observed in the VIS including the extrastriate and inferior extratriate, and the DAN including postcentral regions and superior parietal lobule, as well as the SMN. These reductions were characterized by low-level visual sensory and motor functions involving visual perception, visual attention, motor, action, eye movements, visuospatial, multisensory processing, and reading (**Figure 4B**).

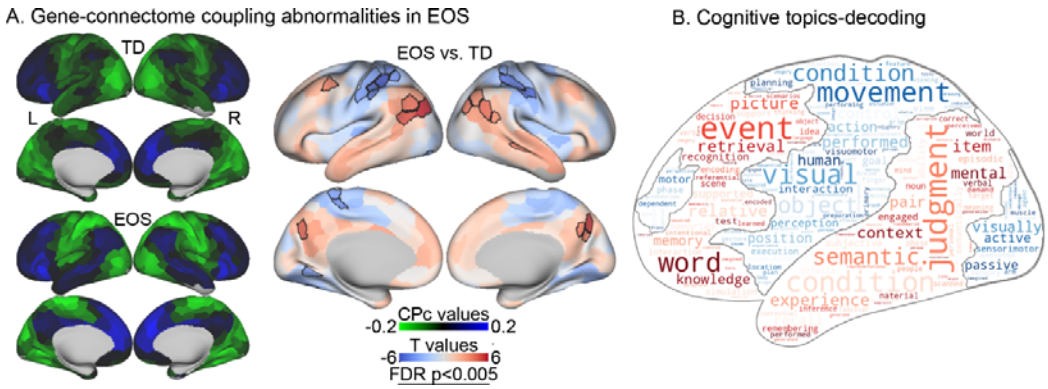

Figure 4. Cognitive relevance of gene-connectome coupling abnormalities in EOS. (A) Parcel-wise couplings between functional connectome and gene expression (CPc) for TD and EOS, and their differences (t-test, EOS vs. TD). Cortical parcels with positive CPc values (blue) indicate as preferential associations with matrix thalamic cells, and negative CPc values (green) suggested core cells. Parcels with significantly different coupling patterns are surrounded by black contours [false discovery rate (FDR) corrections, $p < 0.005$]. **(B)** Topic-based functional decoding of abnormal regions in EOS. Cognitive terms in warm color correspond to brain regions showing hyper-couplings in patients relative to controls, and cool color represents hypo-couplings. In the word cloud, the size of a cognitive term is proportional to the strength of its loading.

Discussion

In the current study we investigated macroscale thalamic functional organization in EOS by employing manifold learning techniques and cytoarchitecture-informed analyses on thalamocortical functional connectivity. We found both expansions along L-M principal axis and A-P secondary axis of thalamic hierarchies in EOS, indicating connectivity profiles between both anchors were more dissimilar. Disordered functional hierarchies of the thalamus were related to altered thalamocortical interactions both in unimodal and transmodal networks. To evaluate the cytoarchitectural underpinnings of the macroscale functional organization disturbances in EOS, we compared alterations in functional organization within core- and matrix-cells that derived from an independent transcriptomic atlas. We found that in particular, functional organization of thalamic core cells was altered in EOS. Moreover, patients' abnormal coupling patterns between a-priori map of the core-matrix cytoarchitecture and functional connectome characterized a spectrum from perceptual to abstract cognitive functions. In sum, the current findings provide mechanistic evidence for disrupted thalamocortical system in EOS, and point to alterations in functional networks associated with both perceptual and cognitive functions.

In line with previous work of thalamic hierarchies (Yang et al., 2020), the principal functional gradient described continuous transition from the ventral lateral nucleus to the anterior and pulvinar groups, and the second axis delineated gradual transition from the anterior nuclei to the pulvinar. Whereas L-M thalamic axis has been reported to correspond to the distribution of gray matter morphology, i.e., low-to-high intensity of neural mass, and

the A-P gradient was strongly related to the intrinsic geometry of the thalamus (Yang et al., 2020). These findings suggested an association between functional thalamic hierarchies and its structure. Albeit not directly shown, L-M and A-P axes might plausibly reflect functional relevance in different dimensions, i.e., two kinds of transitions across functional networks (Yang et al., 2020). In line with their observation, we found that the L-M principal axis functionally segregated unimodal networks, similar to the second gradient of cortical connectome (Margulies et al., 2016). Conversely, the A-P axis of thalamic hierarchies segregated unimodal and transmodal networks, in accord with previous findings (Yang et al., 2020). Taking together, beyond supporting macroscale thalamic hierarchical framework, the current findings further broaden our knowledge of functional specialization of thalamic L-M and A-P axes.

Thalamic ventral lateral and ventral posterior nuclei, as one end of the L-M organizational axis, exhibited evident dissociation in EOS. Both nuclei receive neuronal input from the sensory periphery, and project to the motor and somatosensory cortices, respectively (Ramcharan, Gnadt, & Sherman, 2005). The etiology of schizophrenia has been suggested to damage refinement of motor/somatosensory-thalamic connectivity patterns that occurs during brain maturation (Woodward et al., 2012). Indeed, in adolescent patients relative to adult patients, structural abnormalities in the sensorimotor cortex are reported to be particularly salient (Douaud et al., 2007), but may gradually fade out within a longitudinal period of observation (Douaud et al., 2009). Moreover, motor performance has been reported worse in adolescent patients relative to adult patients when accounting for developmental

factors (White, Ho, Ward, O'Leary, & Andreasen, 2006). In line with this observation, a meta-analysis suggested that motor deficits may precede the onset of schizophrenia and may constitute robust antecedents of this mental disorder (Dickson, Laurens, Cullen, & Hodgins, 2012). In the context, we postulate sensorimotor-related segregation along thalamic L-M hierarchy might underlie premorbid disturbances in motor development, a marker distinct to schizophrenia.

Compared with TD, EOS patients had increased segregation in two extremes of the A-P axis, i.e., visual-related pulvinar nucleus and default mode-associated anterior nuclear group. Weaker functional connectivity between the VIS and DMN has been previously reported in EOS (Hilland et al., 2022; Peng et al., 2021). In fact, given the central role of the thalamus in the development of the cerebral cortex (Lopez-Bendito & Molnar, 2003), abnormalities of the cerebral cortex in schizophrenia might occur secondary to thalamic pathology (Jones, 1997; Selemon et al., 2005). Thus, the unimodal-transmodal thalamic hierarchy expansion might further result in disturbed cortical differentiation of unimodal and transmodal regions in EOS. A cortical hierarchy dissociating sensory from transmodal regions has been implicated in cognitive processing, describing a functional processing axis from perceptual/action towards abstract cognition functions including social cognition and memory (Margulies et al., 2016; Mesulam, 1998). At the same time, a compression of the unimodal-to-transmodal cortical hierarchy was recently found in chronic adult-onset schizophrenia (Debo Dong et al., 2020), in contrast with our findings of expansion. Given age-dependent shifts in the macroscale cortical hierarchy (Dong, Margulies, Zuo, & Holmes,

2021), this inconsistence might due to their disparate stage of the illness and age of onset, or their usage of antipsychotic drugs. Further longitudinal works are needed to chart functional organization abnormalities of the thalamus and the cerebral cortex during the course of schizophrenia. Nevertheless, the current findings embed thalamus into cortical functional hierarchy during cognitive processes, paving the way to comprehensively reveal cognitive defects, another well documented precursor of schizophrenia excepts for motor deficits (Dickson et al., 2012).

Leveraging our observations of alterations of thalamic functional organization against a proxy map of core/matrix cells based on post-mortem transcriptomic data (Muller et al., 2020), we observed thalamic core cells to underlie expansive functional hierarchies in EOS, rather than matrix cells. Core and matrix cells are two primary types of thalamic relay neurons which separately exhibit immunoreactivity to the calcium binding proteins Parvalbumin and Calbindin (Jones, 1998). Thalamic nuclei differ in the ratio of core and matrix neurons (Jones, 2002). Specifically, sensory and motor relay nuclei, as well as the pulvinar nuclei and the intralaminar nuclei are chiefly composed of core cells (Halassa & Sherman, 2019). Compared with matrix cells, the larger core cells innervate middle cortical layers in a more area-restricted and topographically-organized fashion (Jones, 1998). Functionally, Parvalbumin-rich core cells have been reported to act as drivers of feed-forward activity, while Calbindin-rich matrix cells fulfil a more modulatory function (Jones, 2001). Together, this may suggest that thalamic hierarchy disturbances in EOS may relate to the “feed-forward” pathway that transmits information from the sensory periphery,

not the “feed-back” pathway (Garcia-Cabezas, Zikopoulos, & Barbas, 2019). A further inspection of gene-connectome coupling abnormalities in EOS by evaluating the selective connection of the core-matrix cytoarchitecture with the cortex could show that, patients’ core thalamus dys-connected with both unimodal and transmodal cortices. In healthy adults, core regions have preferential connections with unimodal primary regions, and matrix areas with transmodal cortices incorporating the DMN, FPN, VAN and the limbic network (Muller et al., 2020). Conversely in the current pediatric sample, we observed core-related connections with wide-spread cortical regions including both unimodal and posterior transmodal cortices for TD, whereas EOS had lager similarity with the previously reported adult pattern, i.e., stronger core-related couplings in the VIS, SMN and DAN and weaker couplings in the DMN and FPN. Together, our results imply putatively excessive maturation in the thalamocortical feedforward pathway of schizophrenia. However, future molecular-level work is undoubtedly needed to elaborate on the feedforward pathway alterations in the still developing brain of schizophrenia.

Functional decoding of our map of gene-connectome coupling abnormalities in EOS derived a sensory-cognitive behavioral architecture from the gene-connectome coupling pattern, describing functions associated with primary sensory and multisensory processing to working memory, cognitive control and motivation. Along the continuous behavioral spectrum, perception (especially visual sensory), motor, and higher cognition such as memory are particularly affected by schizophrenia. Consistently, thalamic hierarchy abnormalities were sensorimotor-related, as well as visual/ default mode-associated along a

second axis. As the “cognitive dysmetria” theory suggested, the multitude and diversity of behavior deficits in schizophrenia might be tied to an impaired fundamental cognitive process mediated by the thalamus (Andreasen et al., 1996; Andreasen, Paradiso, & O'Leary, 1998). This impairment, i.e., cognitive dysmetria referred to a disruption of the fluid and coordinated sequences of both thought and action, leading to a decreased coordination of perception, retention, retrieval, and response functions (Andreasen, 1999). Furthermore, it has been suggested that schizophrenic brain may not form connections according to gene encoded blueprints which have been phylogenetically determined to be the most efficient (Andreasen et al., 1996). In line with this, our findings reveal gene-connectome coupling abnormalities in the thalamocortical system of EOS and its involvement in cognitive networks, thereby adding new evidence for the “cognitive dysmetria” theory and their genetic inference. However, there is an obvious shortage in our gene-related analyses. The gene expression levels were assessed from post-mortem brain tissue of adults (Hawrylycz et al., 2012), which might be different from the pediatric human brain. Limited by the lack of pediatric transcriptional atlas, our findings about the association between macroscale connectome topology and gene architecture should be carefully considered.

In sum, the current study describes thalamic functional organization abnormalities in early onset schizophrenia, which could be related to “feed-forward” core thalamocortical pathway. Abnormal gene-connectome couplings in the thalamocortical pathway might perturb behaviors involving both low-level perception and high-level cognition, resulting in the diverse profile of symptoms in schizophrenia.

Materials and Methods

Participants

Ninety-nine antipsychotic-naive first-episode EOS patients and 100 typically developing (TD) controls were recruited from the First Hospital of Shanxi Medical University and the local community through advertisements, respectively. All pediatric participants were 7–17 years old and right-handed. The diagnosis of schizophrenia was in accordance with the Structured Clinical Interview for DSM-IV, and was confirmed by senior psychiatrists through a structured clinical interview after at least 6-months of follow-up. The psychiatric symptomatology of 71 patients was evaluated using the Positive and Negative Syndrome Scale (PANSS). Exclusion criteria for all subjects included 1) >= 18 years old; 2) co-morbid Axis-I or Axis-II disease; 3) neurological MRI anomalies; 4) any electronic or metal implants; or 5) substance abuse. In addition, EOS patients were excluded if they suffered from the illness for > 1 year, and TD controls were excluded if they and their first-degree relatives had any history of psychiatric disorder. This retrospective study was approved by the Ethics Committee of the First Hospital of Shanxi Medical University. Written consent was obtained from every participant and their parents or legal guardians.

Four patients and two controls were excluded from the study because of incomplete scanning data, nine patients and six controls due to excessive head motion [mean frame-wise displacement, (FD) > 0.2 mm or outliers > 50%], and one control due to poor quality of intrasubject brain registration. Ultimately, 86 EOS patients (31 men; mean age ± SD = 14.56 ± 1.95 years; mean FD for head motion ± SD = 0.07 ± 0.03 mm) and 91

demographically-matched TD controls (33 men, Chi-square = 0.0009, p = 0.98; mean age ± SD = 14.34 ± 2.02 years, Mann-Whitney U = 3711, p = 0.55; mean FD ± SD = 0.07 ± 0.03 mm, Mann-Whitney U = 3843, p = 0.84) were included in the analysis.

MRI acquisition

Multimodal MRI data were collected using a 3 Tesla MRI scanner (MAGNETOM Verio; Siemens, Germany) in the First Hospital of Shanxi Medical University. T1-weighted data were acquired using a three-dimensional fast spoiled gradient-echo sequence [repetition time (TR) = 2,300 ms; echo time (TE) = 2.95 ms; flip angle = 9°; matrix = 256 × 240; slice thickness = 1.2 mm (no gap); and voxel size = 0.9375 × 0.9375 × 1.2 mm^3, with 160 axial slices]. Resting-state functional MRI (rs-fMRI) data were obtained using a two-dimensional echo-planar imaging sequence [TR = 2,500 ms; TE = 30 ms; flip angle = 90°; matrix = 64 × 64; number of volumes = 198; slice thickness = 3 mm (1 mm gap); and voxel size = 3.75 × 3.75 × 4 mm^3, with 32 axial slices].

MRI processing

T1-weighted structural data were preprocessed with FreeSurfer (v7.1.0, http://surfer.nmr.mgh.harvard.edu/), which included cortical segmentation and surface reconstruction. Rs-fMRI functional data were preprocessed with the CBIG pipeline (https://github.com/ThomasYeoLab/CBIG) based on FSL [v5.0.9, (Woolrich et al., 2009)] and FreeSurfer (v7.1.0), which included removal of the first four volumes, slice-timing, motion correction, and boundary-based registration to structural images. Participants with

the intrasubject registration cost exceeding the 0.7 were discarded. Additionally, subjects with severe segmentation faults were excluded via visual inspection. Volumes with FD > 0.2 mm or voxel-wise differentiated signal variance > 50 were marked as outliers. Censored images included one volume before and two volumes after outliers, as well as images lasting fewer than five contiguous volumes time frames. Participants with a mean FD > 0.2 mm or censored volumes percent > 50% were excluded from all further analyses. Censored images were excluded and substituted by the least square interpolation of neighbor time frames. White matter signal, ventricular signal, head motion parameters and temporal derivatives were regressed out to remove spurious noise affects. Subsequently, functional images were then bandpass filtered (0.01–0.08 Hz). Preprocessed images were then registered to MNI152 template and resampled to the cortical surface using Ciftify package [v2.3.3, (Dickie et al., 2019)]. The thalamus was localized using the Gordon 333 Atlas (Gordon et al., 2016), including 2536 voxels across both hemispheres.

Macroscale thalamic connectome manifolds

Thalamocortical gradients identification

Analogous to previous work (Yang et al., 2020), gradients of thalamocortical functional connectome were generated using the diffusion embedding algorithm in BrainSpace Toolbox (Vos de Wael et al., 2020). First, thalamocortical functional connectomes were calculated based on Pearson correlations between the thalamic and cortical rs-fMRI time-series for each subject (Margulies et al., 2016; Meng et al., 2021). A group representative connectome was calculated by averaging thalamocortical connectomes across patients and controls. Both

individual-level and group-level connectome matrices were then row-wise thresholded (the top 10% connections retained) and converted into cosine similarity matrices (Margulies et al., 2016; Paquola et al., 2019). Subsequently, nonlinear dimensionality reduction techniques were employed on the group-level similarity matrix to resolve a template connectome gradient, i.e., spatial axis in connectome variations (Coifman & Lafon, 2006). Individual gradients were then estimated and aligned to the template gradients. Finally, they were smoothed (FWHM = 5mm) across thalamic voxels to avoid introducing artifactual correlation.

We selected the first two gradients to represent the macroscale thalamic connectome manifolds, which explained 35.9 % of total eigenvariance in functional connectome. To quantify the dispersion of each thalamic voxel in the two-dimensional gradient space, we computed manifold eccentricity, i.e., the square root of the Euclidian distance from each thalamic voxel to the center of mass in the two-dimensional gradient space for each individual (Park et al., 2021). For each participant, global eccentricity was calculated by averaging eccentricity values across all thalamic voxels, indicating overall dispersion of the gradient space.

Thalamic functional community division

To characterize the network-level relevance of macroscale thalamic connectome manifolds, we created a thalamic functional atlas using winner-take-all representation approach (Yang et al., 2020). The winner-take-all representations are efficient and generally accurate, due to

most thalamic voxels have strong correlation with only one cortical region (D. Zhang et al., 2008). Partial correlations were computed between rs-fMRI time-series of each thalamic voxel and six intrinsic cortical networks (Yeo et al., 2011) including the visual network (VIS), sensorimotor network (SMN), dorsal attention network (DAN), ventral attention network (VAN), frontoparietal network (FPN), and default mode network (DMN). The limbic network was excluded for low signal quality in corresponding cortical areas of our data. Each thalamic voxel was labeled by the cortical network showing the highest partial correlation coefficient.

The core-matrix cytoarchitecture

Linking thalamic core-matrix cytoarchitecture with connectome manifolds

To delineate the core-matrix cytoarchitecture in the thalamus, we used the spatial maps of mRNA expression levels for two calcium-binding proteins (CALB1 and PVALB) (https://github.com/macshine/corematrix) generated from post-mortem Allen Human Brain Atlas (Hawrylycz et al., 2012). Two (CUST_11451_PI416261804 and A_23_P17844) and three probes (CUST_140_PI416408490, CUST_16773_PI416261804 and A_23_P43197) were used to estimate the gene expressions of PVALB and CALB1, respectively (Muller et al., 2020). Expression differences between normalized CALB1 and PVALB levels denoted CPt index, i.e., CALB1-PVALB values for thalamic voxels. Thalamic voxels with positive CPt values related to matrix projection cells, and voxels with negative values related to core populations. Global eccentricity indices of core/matrix populations were separately measured by averaging eccentricity values across all thalamic core/matrix cells, and

compared with each other.

Subsequently, we sought to reveal an association between the thalamic cytoarchitecture and disturbed connectome manifold in EOS patients. Between-group difference map of eccentricity was used as quantification index for perturbances of macroscale connectome gradients. Spatial correlations were employed between gene expression maps and differential eccentricity map between the EOS and TD groups. To correct for the spatial autocorrelation (SA) of brain maps, we employed the variogram-matching model to simulated surrogate maps (N = 1,000) preserving SA of empirical volumetric maps (Burt, Helmer, Shinn, Anticevic, & Murray, 2020). These surrogate maps were then used as null distributions for evaluating SA-corrected statistical significance.

Functional decoding of cytoarchitecture-connectome couplings

To estimate cognitive implications of couplings between core-matrix cytoarchitecture and functional connectome, we projected CPt maps onto the cerebral cortex (i.e., CPc maps). For each subject, CPc map was computed by spatially correlating CPt map and thalamocortical connectome (Muller et al., 2020), and were then down sampled into 400 cortical parcels according to the Schaefer atlas (Schaefer et al., 2018). Cortical parcels with positive CPc values indicated as preferential associations with matrix thalamic populations, and negative values suggested core populations. Next, topic-based functional decoding was conducted to evaluate cognitive terms associated with CPc maps using NeuroSynth meta-analytic database (Yarkoni et al., 2011). Topics were derived from the 50-set topic, where 6 topics

were removed as "noise" according to a previous study (Margulies et al., 2016). CPc map with significant group differences between patients and controls was binarized for creating regions of interest (ROIs) masks in the meta-analyses. This analysis was constrained in the 21 cognitive topics significantly associated with CPc maps (z−statistic > 3.1, see supplement for further information). To better visualize our result, we generated a word cloud (https://amueller.github.io/word_cloud/) summarizing frequency of all cognitive terms included in associated topics as previously suggested (Vogel et al., 2020). The size of a cognitive term in the word cloud is proportional to the strength of its loading.

Group comparisons between the EOS and TD groups

Between-group differences on all kinds of measurements were assessed by using two-sample t-tests with covariates including age, gender, and mean FD. The multiple comparison corrections were conducted using three methods for different spatial scales: voxel-wise, parcel-wise, and global-wise. For voxel-wise thalamic gradient and eccentricity values, multiple comparison corrections were employed using the permutation-based threshold-free cluster enhancement (TFCE, 10,000 permutations, $p < 0.005$) method (FSL-PALM), which could improve sensitivity and interpretable than cluster-based thresholding method (Smith & Nichols, 2009). For parcel-wise CPc values, false discovery rate (FDR) corrections ($p < 0.005$) were used to control the effect of false positives. For global-wise index like network-level gradient values and global eccentricity values, Bonferroni corrections were conducted with a significant level of $p < 0.05$.

Acknowledgements

We are grateful to all the participants and their guardians in this study. This work was supported by the National Natural Science Foundation of China (82121003, 62036003, 62073058, 62173070), Innovation Team and Talents Cultivation Program of National Administration of Traditional Chinese Medicine (ZYYCXTD-D-202003). S.L.V. was also funded in part by Helmholtz Association's Initiative and Networking Fund under the Helmholtz International Lab grant agreement InterLabs-0015, and the Canada First Research Excellence Fund (CFREF Competition 2, 2015-2016) awarded to the Healthy Brains, Healthy Lives initiative at McGill University, through the Helmholtz International BigBrain Analytics and Learning Laboratory (HIBALL). The authors declare that they have no conflict of interest.

References

Andreasen, N. C. (1999). A unitary model of schizophrenia: Bleuler's "fragmented phrene" as schizencephaly. *Arch Gen Psychiatry, 56*(9), 781-787. doi: 10.1001/archpsyc.56.9.781

Andreasen, N. C., O'Leary, D. S., Cizadlo, T., Arndt, S., Rezai, K., Ponto, L. L., . . . Hichwa, R. D. (1996). Schizophrenia and cognitive dysmetria: a positron-emission tomography study of dysfunctional prefrontal-thalamic-cerebellar circuitry. *Proc Natl Acad Sci U S A, 93*(18), 9985-9990. doi: 10.1073/pnas.93.18.9985

Andreasen, N. C., Paradiso, S., & O'Leary, D. S. (1998). "Cognitive dysmetria" as an integrative theory of schizophrenia: a dysfunction in cortical-subcortical-cerebellar circuitry? *Schizophr Bull, 24*(2), 203-218. doi: 10.1093/oxfordjournals.schbul.a033321

Bayrak, S., Khalil, A. A., Villringer, K., Fiebach, J. B., Villringer, A., Margulies, D. S., & Ovadia-Caro, S. (2019). The impact of ischemic stroke on connectivity gradients. *Neuroimage Clin, 24*, 101947. doi: 10.1016/j.nicl.2019.101947

Burt, J. B., Helmer, M., Shinn, M., Anticevic, A., & Murray, J. D. (2020). Generative modeling of brain maps with spatial autocorrelation. *Neuroimage, 220*, 117038. doi: 10.1016/j.neuroimage.2020.117038

Coifman, R. R., & Lafon, S. (2006). Diffusion maps. *Applied and Computational Harmonic Analysis, 21*(1), 5-30. doi: https://doi.org/10.1016/j.acha.2006.04.006

Dickie, E. W., Anticevic, A., Smith, D. E., Coalson, T. S., Manogaran, M., Calarco, N., . . . Voineskos, A. N. (2019). Ciftify: A framework for surface-based analysis of legacy

MR acquisitions. *Neuroimage, 197*, 818-826. doi: 10.1016/j.neuroimage.2019.04.078

Dickson, H., Laurens, K. R., Cullen, A. E., & Hodgins, S. (2012). Meta-analyses of cognitive and motor function in youth aged 16 years and younger who subsequently develop schizophrenia. *Psychol Med, 42*(4), 743-755. doi: 10.1017/S0033291711001693

Dong, D., Luo, C., Guell, X., Wang, Y., He, H., Duan, M., . . . Yao, D. (2020). Compression of Cerebellar Functional Gradients in Schizophrenia. *Schizophr Bull*. doi: 10.1093/schbul/sbaa016

Dong, D., Yao, D., Wang, Y., Hong, S.-J., Genon, S., Xin, F., . . . Luo, C. (2020). Altered Sensorimotor-to-Transmodal Hierarchical Organization in Schizophrenia. *bioRxiv*, 2020.2003.2006.980607. doi: 10.1101/2020.03.06.980607

Dong, H. M., Margulies, D. S., Zuo, X. N., & Holmes, A. J. (2021). Shifting gradients of macroscale cortical organization mark the transition from childhood to adolescence. *Proc Natl Acad Sci U S A, 118*(28). doi: 10.1073/pnas.2024448118

Douaud, G., Mackay, C., Andersson, J., James, S., Quested, D., Ray, M. K., . . . James, A. (2009). Schizophrenia delays and alters maturation of the brain in adolescence. *Brain, 132*(Pt 9), 2437-2448. doi: 10.1093/brain/awp126

Douaud, G., Smith, S., Jenkinson, M., Behrens, T., Johansen-Berg, H., Vickers, J., . . . James, A. (2007). Anatomically related grey and white matter abnormalities in adolescent-onset schizophrenia. *Brain, 130*(Pt 9), 2375-2386. doi: 10.1093/brain/awm184

Garcia-Cabezas, M. A., Zikopoulos, B., & Barbas, H. (2019). The Structural Model: a theory linking connections, plasticity, pathology, development and evolution of the cerebral

cortex. *Brain Struct Funct, 224*(3), 985-1008. doi: 10.1007/s00429-019-01841-9

Gordon, E. M., Laumann, T. O., Adeyemo, B., Huckins, J. F., Kelley, W. M., & Petersen, S. E. (2016). Generation and Evaluation of a Cortical Area Parcellation from Resting-State Correlations. *Cereb Cortex, 26*(1), 288-303. doi: 10.1093/cercor/bhu239

Halassa, M. M., & Sherman, S. M. (2019). Thalamocortical Circuit Motifs: A General Framework. *Neuron, 103*(5), 762-770. doi: 10.1016/j.neuron.2019.06.005

Hawrylycz, M. J., Lein, E. S., Guillozet-Bongaarts, A. L., Shen, E. H., Ng, L., Miller, J. A., . . . Jones, A. R. (2012). An anatomically comprehensive atlas of the adult human brain transcriptome. *Nature, 489*(7416), 391-399. doi: 10.1038/nature11405

Hilland, E., Johannessen, C., Jonassen, R., Alnaes, D., Jorgensen, K. N., Barth, C., . . . Agartz, I. (2022). Aberrant default mode connectivity in adolescents with early-onset psychosis: A resting state fMRI study. *Neuroimage Clin, 33*, 102881. doi: 10.1016/j.nicl.2021.102881

Hong, S. J., Vos de Wael, R., Bethlehem, R. A. I., Lariviere, S., Paquola, C., Valk, S. L., . . . Bernhardt, B. C. (2019). Atypical functional connectome hierarchy in autism. *Nat Commun, 10*(1), 1022. doi: 10.1038/s41467-019-08944-1

Huntenburg, J. M., Bazin, P. L., & Margulies, D. S. (2018). Large-Scale Gradients in Human Cortical Organization. *Trends Cogn Sci, 22*(1), 21-31. doi: 10.1016/j.tics.2017.11.002

Hwang, K., Bertolero, M. A., Liu, W. B., & D'Esposito, M. (2017). The Human Thalamus Is an Integrative Hub for Functional Brain Networks. *J Neurosci, 37*(23), 5594-5607. doi: 10.1523/JNEUROSCI.0067-17.2017

Jacobsen, L. K., & Rapoport, J. L. (1998). Research update: childhood-onset schizophrenia:

implications of clinical and neurobiological research. *J Child Psychol Psychiatry, 39*(1), 101-113.

Jones, E. G. (1997). Cortical development and thalamic pathology in schizophrenia. *Schizophr Bull, 23*(3), 483-501. doi: 10.1093/schbul/23.3.483

Jones, E. G. (1998). Viewpoint: the core and matrix of thalamic organization. *Neuroscience, 85*(2), 331-345. doi: 10.1016/s0306-4522(97)00581-2

Jones, E. G. (2001). The thalamic matrix and thalamocortical synchrony. *Trends Neurosci, 24*(10), 595-601. doi: 10.1016/s0166-2236(00)01922-6

Jones, E. G. (2002). Thalamic circuitry and thalamocortical synchrony. *Philos Trans R Soc Lond B Biol Sci, 357*(1428), 1659-1673. doi: 10.1098/rstb.2002.1168

Jones, E. G. (2009). Synchrony in the interconnected circuitry of the thalamus and cerebral cortex. *Ann N Y Acad Sci, 1157*, 10-23. doi: 10.1111/j.1749-6632.2009.04534.x

Kinney, D. K., & Matthysse, S. (1978). Genetic transmission of schizophrenia. *Annu Rev Med, 29*, 459-473. doi: 10.1146/annurev.me.29.020178.002331

Lopez-Bendito, G., & Molnar, Z. (2003). Thalamocortical development: how are we going to get there? *Nat Rev Neurosci, 4*(4), 276-289. doi: 10.1038/nrn1075

Margulies, D. S., Ghosh, S. S., Goulas, A., Falkiewicz, M., Huntenburg, J. M., Langs, G., . . . Smallwood, J. (2016). Situating the default-mode network along a principal gradient of macroscale cortical organization. *Proc Natl Acad Sci U S A, 113*(44), 12574-12579. doi: 10.1073/pnas.1608282113

Meng, Y., Yang, S., Chen, H., Li, J., Xu, Q., Zhang, Q., . . . Liao, W. (2021). Systematically disrupted functional gradient of the cortical connectome in generalized epilepsy:

Initial discovery and independent sample replication. *Neuroimage, 230*, 117831. doi: 10.1016/j.neuroimage.2021.117831

Mesulam, M. M. (1998). From sensation to cognition. *Brain, 121 (Pt 6)*, 1013-1052. doi: 10.1093/brain/121.6.1013

Muller, E. J., Munn, B., Hearne, L. J., Smith, J. B., Fulcher, B., Arnatkeviciute, A., . . . Shine, J. M. (2020). Core and matrix thalamic sub-populations relate to spatio-temporal cortical connectivity gradients. *Neuroimage, 222*, 117224. doi: 10.1016/j.neuroimage.2020.117224

Nakagawa, Y. (2019). Development of the thalamus: From early patterning to regulation of cortical functions. *Wiley Interdiscip Rev Dev Biol, 8*(5), e345. doi: 10.1002/wdev.345

Paquola, C., Vos De Wael, R., Wagstyl, K., Bethlehem, R. A. I., Hong, S. J., Seidlitz, J., . . . Bernhardt, B. C. (2019). Microstructural and functional gradients are increasingly dissociated in transmodal cortices. *PLoS Biol, 17*(5), e3000284. doi: 10.1371/journal.pbio.3000284

Park, B. Y., Bethlehem, R. A., Paquola, C., Lariviere, S., Rodriguez-Cruces, R., Vos de Wael, R., . . . Bernhardt, B. C. (2021). An expanding manifold in transmodal regions characterizes adolescent reconfiguration of structural connectome organization. *Elife, 10*. doi: 10.7554/eLife.64694

Peng, Y., Zhang, S., Zhou, Y., Song, Y., Yang, G., Hao, K., . . . Zhang, Y. (2021). Abnormal functional connectivity based on nodes of the default mode network in first-episode drug-naive early-onset schizophrenia. *Psychiatry Res, 295*, 113578. doi: 10.1016/j.psychres.2020.113578

Pergola, G., Selvaggi, P., Trizio, S., Bertolino, A., & Blasi, G. (2015). The role of the thalamus in schizophrenia from a neuroimaging perspective. *Neurosci Biobehav Rev, 54*, 57-75. doi: 10.1016/j.neubiorev.2015.01.013

Ramcharan, E. J., Gnadt, J. W., & Sherman, S. M. (2005). Higher-order thalamic relays burst more than first-order relays. *Proc Natl Acad Sci U S A, 102*(34), 12236-12241. doi: 10.1073/pnas.0502843102

Schaefer, A., Kong, R., Gordon, E. M., Laumann, T. O., Zuo, X. N., Holmes, A. J., . . . Yeo, B. T. T. (2018). Local-Global Parcellation of the Human Cerebral Cortex from Intrinsic Functional Connectivity MRI. *Cereb Cortex, 28*(9), 3095-3114. doi: 10.1093/cercor/bhx179

Selemon, L. D., Wang, L., Nebel, M. B., Csernansky, J. G., Goldman-Rakic, P. S., & Rakic, P. (2005). Direct and indirect effects of fetal irradiation on cortical gray and white matter volume in the macaque. *Biol Psychiatry, 57*(1), 83-90. doi: 10.1016/j.biopsych.2004.10.014

Shine, J. M. (2021). The thalamus integrates the macrosystems of the brain to facilitate complex, adaptive brain network dynamics. *Prog Neurobiol, 199*, 101951. doi: 10.1016/j.pneurobio.2020.101951

Smith, S. M., & Nichols, T. E. (2009). Threshold-free cluster enhancement: addressing problems of smoothing, threshold dependence and localisation in cluster inference. *Neuroimage, 44*(1), 83-98. doi: 10.1016/j.neuroimage.2008.03.061

Stephan, K. E., Friston, K. J., & Frith, C. D. (2009). Dysconnection in schizophrenia: from abnormal synaptic plasticity to failures of self-monitoring. *Schizophr Bull, 35*(3),

509-527. doi: 10.1093/schbul/sbn176

Valk, S. L., Xu, T., Paquola, C., Park, B.-y., Bethlehem, R. A. I., Vos de Wael, R., . . . Bernhardt, B. C. (2021). Genetic and phylogenetic uncoupling of structure and function in human transmodal cortex. *bioRxiv*, 2021.2006.2008.447522. doi: 10.1101/2021.06.08.447522

Vazquez-Rodriguez, B., Suarez, L. E., Markello, R. D., Shafiei, G., Paquola, C., Hagmann, P., . . . Misic, B. (2019). Gradients of structure-function tethering across neocortex. *Proc Natl Acad Sci U S A, 116*(42), 21219-21227. doi: 10.1073/pnas.1903403116

Vogel, J. W., La Joie, R., Grothe, M. J., Diaz-Papkovich, A., Doyle, A., Vachon-Presseau, E., . . . Evans, A. C. (2020). A molecular gradient along the longitudinal axis of the human hippocampus informs large-scale behavioral systems. *Nat Commun, 11*(1), 960. doi: 10.1038/s41467-020-14518-3

Vos de Wael, R., Benkarim, O., Paquola, C., Lariviere, S., Royer, J., Tavakol, S., . . . Bernhardt, B. C. (2020). BrainSpace: a toolbox for the analysis of macroscale gradients in neuroimaging and connectomics datasets. *Commun Biol, 3*(1), 103. doi: 10.1038/s42003-020-0794-7

White, T., Ho, B. C., Ward, J., O'Leary, D., & Andreasen, N. C. (2006). Neuropsychological performance in first-episode adolescents with schizophrenia: a comparison with first-episode adults and adolescent control subjects. *Biol Psychiatry, 60*(5), 463-471. doi: 10.1016/j.biopsych.2006.01.002

Woodward, N. D., & Heckers, S. (2016). Mapping Thalamocortical Functional Connectivity in Chronic and Early Stages of Psychotic Disorders. *Biol Psychiatry, 79*(12), 1016-1025.

doi: 10.1016/j.biopsych.2015.06.026

Woodward, N. D., Karbasforoushan, H., & Heckers, S. (2012). Thalamocortical dysconnectivity in schizophrenia. *Am J Psychiatry, 169*(10), 1092-1099. doi: 10.1176/appi.ajp.2012.12010056

Woolrich, M. W., Jbabdi, S., Patenaude, B., Chappell, M., Makni, S., Behrens, T., . . . Smith, S. M. (2009). Bayesian analysis of neuroimaging data in FSL. *Neuroimage, 45*(1 Suppl), S173-186. doi: 10.1016/j.neuroimage.2008.10.055

Yang, S., Meng, Y., Li, J., Li, B., Fan, Y. S., Chen, H., & Liao, W. (2020). The thalamic functional gradient and its relationship to structural basis and cognitive relevance. *Neuroimage, 218*, 116960. doi: 10.1016/j.neuroimage.2020.116960

Yarkoni, T., Poldrack, R. A., Nichols, T. E., Van Essen, D. C., & Wager, T. D. (2011). Large-scale automated synthesis of human functional neuroimaging data. *Nat Methods, 8*(8), 665-670. doi: 10.1038/nmeth.1635

Yeo, B. T., Krienen, F. M., Sepulcre, J., Sabuncu, M. R., Lashkari, D., Hollinshead, M., . . . Buckner, R. L. (2011). The organization of the human cerebral cortex estimated by intrinsic functional connectivity. *J Neurophysiol, 106*(3), 1125-1165. doi: 10.1152/jn.00338.2011

Zhang, D., Snyder, A. Z., Fox, M. D., Sansbury, M. W., Shimony, J. S., & Raichle, M. E. (2008). Intrinsic functional relations between human cerebral cortex and thalamus. *J Neurophysiol, 100*(4), 1740-1748. doi: 10.1152/jn.90463.2008

Zhang, M., Palaniyappan, L., Deng, M., Zhang, W., Pan, Y., Fan, Z., . . . Pu, W. (2021). Abnormal Thalamocortical Circuit in Adolescents With Early-Onset Schizophrenia. *J*

Am Acad Child Adolesc Psychiatry, 60(4), 479-489. doi: 10.1016/j.jaac.2020.07.903

SUPPLEMENTARY MATERIALS

Cognitive implications of gene-connectome couplings across all subjects

To estimate cognitive implications of couplings between core-matrix cytoarchitecture and functional connectome, we first projected CPt maps onto the cerebral cortex (i.e., CPc maps). Next, topic-based functional decoding was conducted to evaluate cognitive terms associated with CPc maps using NeuroSynth meta-analytic database. The mean CPc map across all subjects was divided into five-percentile bins and binarized for creating regions of interest (ROIs) masks in the meta-analyses. Topics were derived from the 50-set topic, where 6 topics were removed as "noise" according to a previous study (Margulies et al., 2016). Twenty-one cognitive topics remained after thresholding of z−statistic > 3.1. Core populations preferentially linked with unimodal primary regions that subserve primary sensory and multisensory functions, and matrix areas to transmodal cortices characterized by more abstract cognition (**Figure S1**), suggesting a sensory-cognitive behavioral architecture. Along the continuous spectrum, cognitive consequences shifted from primary sensory and multisensory processing to working memory, cognitive control and motivation.

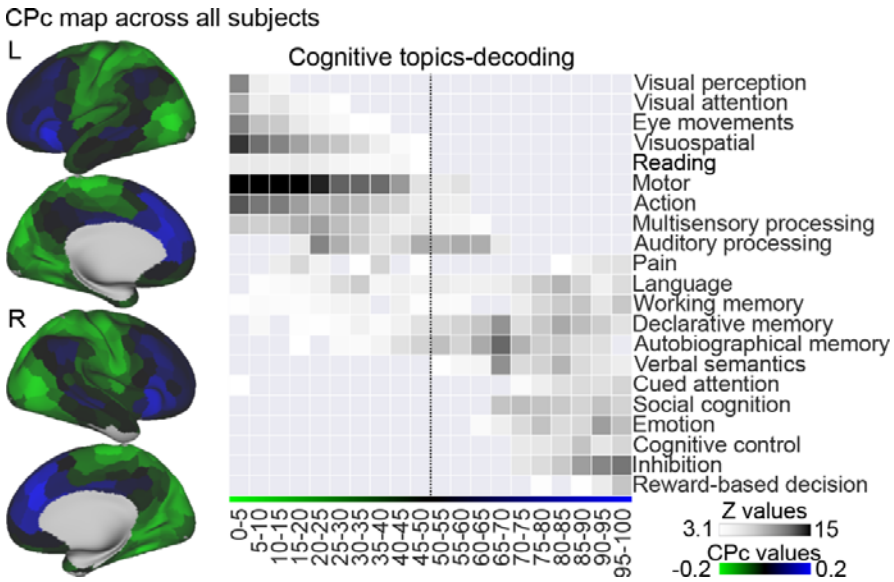

Figure S1. Cognitive consequences of gene-connectome coupling. Parcel-wise Cpc map (left) was obtained using all subjects including patients and controls. In right panel, each cell is colored according to their z-statistic values. Each row represents a cognitive topic, and each column represents a five-percentile bin of CPc mask. Dotted line depicts where CPc value is equal to zero.

References

Margulies, D. S., Ghosh, S. S., Goulas, A., Falkiewicz, M., Huntenburg, J. M., Langs, G., . . . Smallwood, J. (2016). Situating the default-mode network along a principal gradient of macroscale cortical organization. *Proc Natl Acad Sci U S A, 113*(44), 12574-12579. doi: 10.1073/pnas.1608282113